

Real-Time Spectroscopy of the Excited-State Excitons in Porphyrin J-Aggregates

Hideaki Kano[#] and Takayoshi Kobayashi^{*}

Department of Physics, The University of Tokyo, Hongo 7-3-1, Bunkyo-ku, Tokyo 113-0033

(Received October 2, 2001)

The excited exciton (S_2 -exciton originating from the second-excited state of the molecules) was studied by real-time spectroscopy with 30-fs pulses. The ultrafast dynamics due to the S_2 - S_1 internal conversion process were clearly observed in the pump–probe signal. The signal was modulated by the coherent molecular vibrations with $241 \pm 4 \text{ cm}^{-1}$ and $319 \pm 4 \text{ cm}^{-1}$ frequencies. The phase of the oscillation indicates that not only the ground state but also the excited state contribute to the oscillatory signal. The excited-state wave-packet motion was explained by dynamic intensity borrowing mechanism from the $S_2 \rightleftharpoons S_0$ -transitions to the $S_1 \rightleftharpoons S_0$ -transitions.

Femtosecond real-time spectroscopy has attracted much attention because of its capability to probe coherent vibrational dynamics in molecular^{1,2} and condensed matter systems.³ Owing to the broadband laser pulses, the vibrational manifold in the excited state or the ground state is simultaneously photoexcited by the pump pulse and the resultant vibrational wave packet can be monitored by the probe pulse in the time domain. In comparison with stationary and time-resolved Raman spectroscopies, real-time spectroscopy is unique method because the phase of the oscillation can be directly determined from the pump–probe transient traces. Recent development of ultrafast science allows us to observe molecular vibrations with frequencies higher than 2000 cm^{-1} using sub-5-fs laser pulses in time domain.⁴ Such an ultrashort laser pulse was also developed by our group⁵ and was applied to the real-time spectroscopy of the polydiacetylene,⁴ metal–halogen complex,⁶ molecular J-aggregates,⁷ and bacteriorhodopsin.⁸ Although the wave-packet motion is widely observed, there are only a few investigations^{4,9} including theoretical works^{10,11} about the wave-packet dynamics on the potential energy surface (PES) of a higher excited state (for instance, S_2 -state) than the lowest-excited state. This is because the relaxation mechanism such as an internal conversion (IC) is believed to destroy the vibrational coherence. The effect of the IC on the vibrational coherence can be investigated by the femtosecond real-time spectroscopy because of its high time-resolution. Recently, Mataga et al. have carried out detailed investigations of fluorescence up-conversion spectroscopy on free-base tetraphenylporphyrin monomers photogenerated by the S_2 -excitation and have observed an oscillating fluorescence component ($30\text{--}40 \text{ cm}^{-1}$) at a slightly higher photon energy than the S_1 -state peak.⁹ This suggests a coherent vibrational motion on the S_1 -state PES even after the rapid $S_2 \rightarrow S_1$ IC process. The wave-packet dynamics in the S_2 manifold is considered to be more complex than that in the S_1 -state because the ultrafast IC may disturb

the molecular vibrations. In contrast with the molecular system, the influence of the IC process upon the vibrational coherence in the aggregate system has never been examined. Since the stationary absorption spectrum of the porphyrin J-aggregates is well characterized by S_2 - and S_1 -exciton states, the coupling of each exciton with the molecular vibration can be separately evaluated.

In the present study, we have studied the wave-packet dynamics in the presence of the IC. The population relaxation of the excitons and the vibrational dephasing of the porphyrin J-aggregates are investigated by 30-fs pump–probe spectroscopy.

Experimental

The pump–probe experimental setups for monochromatic and polychromatic detections are described elsewhere.⁷ Here only the important parameters of the two experimental systems are described. The pump and probe beams were focused on the sample by spherical mirrors with $r = 200$ - and $r = 300$ -mm curvatures, respectively, with the inter-beam angle of $\sim 3^\circ$ to minimize the reduction of time resolution due to the time-smearing effect. In the present study, laser pulses from a noncollinear optical parametric amplifier (NOPA)⁵ was adjusted to resonantly generate S_2 -exciton. In order to avoid reflection loss and additional wavelength-dependent phase delays around 500 nm, a pair of the chirped mirrors was replaced by an Ag-mirror pair. Typical values of duration, pulse energy, photon energy, and peak wavelength were 30 fs, 18 nJ, 5.9×10^{14} photon/cm², and 506 nm, respectively. The laser pulses were characterized by the frequency-resolved optical gating (FROG) technique.¹² The time-bandwidth product was about 0.55.

Tetrakis(*p*-sulfonylphenyl)porphyrin (TSPP; Tokyo Kasei) was used without further purification. The sample was an aqueous solution of porphyrin J-aggregates in a homemade 250 μm -thick cell. In order to enhance the aggregation, KCl was added to increase the ionic strength. The concentrations of the TSPP and KCl were 10^{-4} and 10^{-1} mol/L, respectively. All measurements were performed at room temperature (298 K).

[#] Present address: Department of Chemistry, The University of Tokyo, Hongo 7-3-1, Bunkyo-ku, Tokyo 113-0033

Results and Discussion

Time-Resolved Difference Absorption Spectrum. Figure 1 shows the stationary absorption spectrum of the porphyrin J-aggregates and the laser spectrum. The absorption spectrum of the J-aggregate is characterized by two bands, the B-band (S_2 -exciton state; $\hbar\omega_{\max} = 2.53$ eV) and the Q-band (S_1 -exciton state; $\hbar\omega_{\max} = 1.75$ eV). The laser spectrum matches the red side of the B-band, therefore the S_2 -exciton can be resonantly photogenerated. The spectral bandwidth of the 30-fs laser pulse was about 20 nm, which corresponds to 807 cm^{-1} and is broad enough to excite several vibrational manifolds in the B-band. Figure 2 shows a three-dimensional plot of the time-resolved difference absorption spectrum as functions of the probe-photon energy and the delay time between the pump and probe pulses. From this three-dimensional plot, a number of features are evident. First, the bleaching signal is clearly observed around the B-band. Secondly, a coherent spike is dominant around the zero-delay time. Finally, weak high-frequency oscillations are superposed on the temporal profile. In order to investigate this oscillating component in more detail,

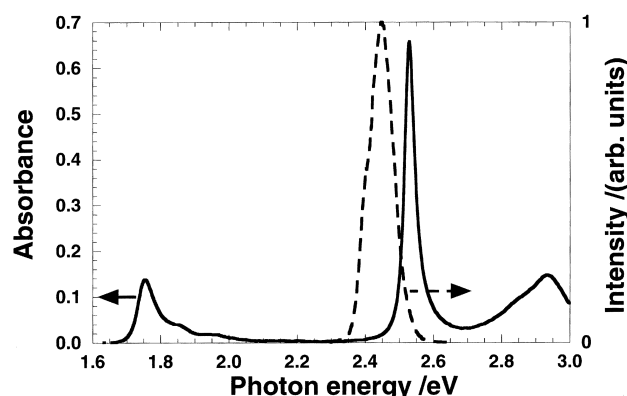


Fig. 1. Stationary absorption spectrum of the TSPP J-aggregates (solid) and laser spectrum (dashed).

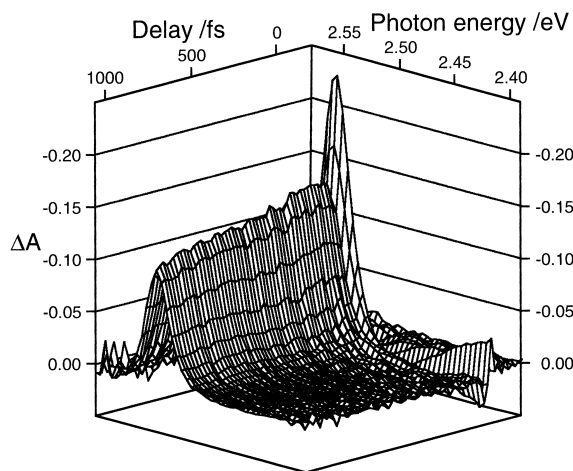


Fig. 2. Three-dimensional plot of the time-resolved difference absorption spectrum of TSPP J-aggregates as functions of probe-photon energy and delay time.

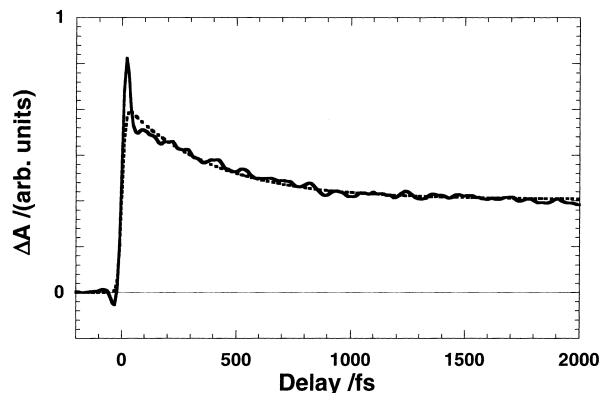


Fig. 3. Delay-time dependence of the induced absorption change of TSPP J-aggregates (solid) and fitted result (dashed)

we attempted monochromatic detection. Figure 3 shows the delay-time dependence of the difference absorption signal (solid) at 2.51 eV. The temporal profile was fitted with use of the following equation;

$$\Delta A(t) = A \exp(-t/\tau) + B \quad (1)$$

Since a coherent spike contributes to the signal around the zero-delay time, it was excluded in the process of the fitting. The decay-time constant was determined to be 380 ± 10 fs. This is consistent with the relaxation time (~ 300 fs) of the $S_2 \rightarrow S_1$ internal conversion (IC) determined previously by time-resolved fluorescence and absorption spectroscopy using 100-fs-laser pulses.¹³ Hence, component A is attributed to the bleaching of the $S_2 \rightleftharpoons S_0$ -transitions. It is noted that component A in the bleaching originates from both the S_2 -exciton-state population and the ground-state depopulation. The ground-state depopulation remains even after the S_2 -exciton converts to the S_1 -exciton, therefore it still gives rise to the bleaching signal. The bleaching signal intensity after the $S_2 \rightarrow S_1$ IC does not decay in the time range of the measurement because the S_1 -exciton lifetime is 295 ps.¹⁴ The component B in Eq. 1 is thus ascribed to this process. Since the probe laser spectrum does not cover the whole spectral range of the B-band (See Fig. 1), especially on the blue side, the photo-induced absorption (PIA) due to the transition between two multi-exciton states of the S_2 -exciton $|n+1, S_2\rangle \leftarrow |n, S_2\rangle$ ($n = 1, 2, \dots$) was not detected, in contrast with the previous study.⁷

Analysis of Coherent Molecular Vibration. As shown in Fig. 3, the oscillating component is also contributing to the signal in the transient traces. In order to extract the oscillating component from the trace, the fitted result (dashed curve in Fig. 3) was subtracted from the raw data (solid in Fig. 3). The resultant oscillating component is Fourier-transformed. Figure 4(a) shows the Fourier power spectrum calculated from Fig. 3 based on the above-mentioned procedure. There are mainly two peaks, namely $241 \pm 4\text{ cm}^{-1}$ and $319 \pm 4\text{ cm}^{-1}$. These peaks are in excellent agreement with the stationary Raman spectrum depicted in Fig. 4(b). Therefore, $241 \pm 4\text{ cm}^{-1}$ and $319 \pm 4\text{ cm}^{-1}$ are assigned to a ruffling and a doming modes, respectively.¹⁴ Note that the signal intensity of the doming mode is more prominent than the one obtained by the S_1 -reso-

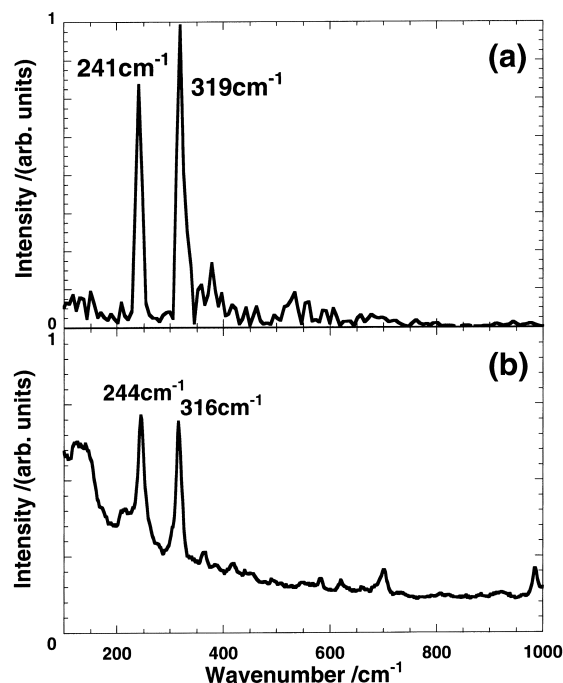


Fig. 4. (a) Fourier-power spectrum of the oscillating component in Fig. 3; (b) Resonance Raman spectrum of TSPP J-aggregates. The excitation wavelength is 488 nm.

nant excitation.⁷ This may be due to a different coupling property of the S₁- and S₂-excitons with each vibrational mode.

The important point to note is that the oscillating component persists for a longer time than the S₂-exciton lifetime (380 ± 10 fs). In order to interpret this result, following two models must be considered. The one is the wave-packet motion prepared on the ground-state PES. It is well known as impulsive stimulated Raman scattering (ISRS).¹⁵ The other is the wave-packet motion prepared on the S₂- and S₁-excited-state PESs. In order to separate these contributions, the phase of the oscillation has been examined by several groups^{16,17,18,19} including an analysis of the probe-photon energy dependence.^{17,18,19} Thus, the key is the phase of the oscillation in the transient trace. Figure 5 shows the phase and amplitude spectra of the ruffling and the doming modes, which are calculated from Fig. 2 with use of the complex Fourier transformation. The phase, ϕ , is defined as $\cos(\Omega t + \phi)$, where Ω represents the vibrational frequency. For both vibrational modes, the amplitudes of the oscillations have the peaks around the B-band and the phases of the oscillations show flat spectra. In addition, the amount of the phases are different between these two modes. Such spectra cannot be explained by the conventional wave-packet motion on the excited-state PES or on the ground-state PES, because each different probe-photon energy probes a different position of the normal coordinate.^{17,18,19} Especially, in the case of the resonant ISRS process, the phases of the oscillations with 241 ± 4 cm⁻¹- and 319 ± 4 cm⁻¹-frequencies are clearly different from the one reported in Refs. 17 and 18. For in-depth analysis of the phase, the oscillating component of the induced absorption signal in Fig. 3 is fitted to the sum of the damped oscillation using a linear predictive singular value decomposition method²⁰ which simultaneously determines both

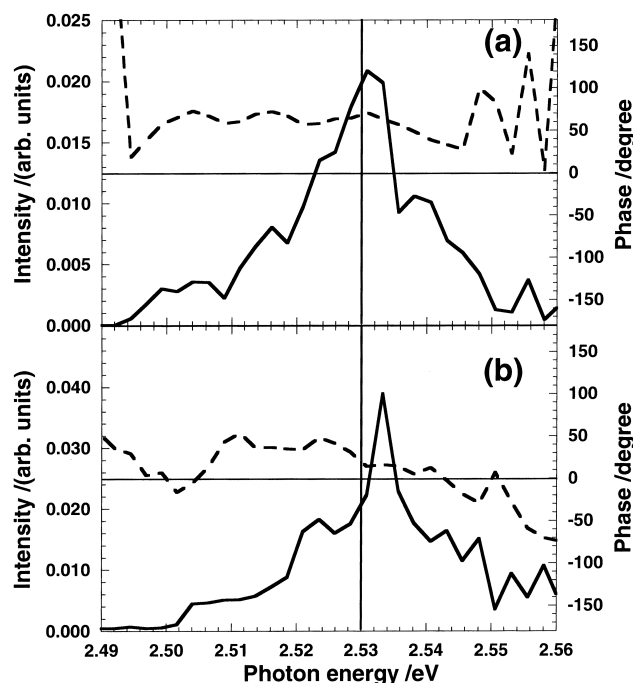


Fig. 5. Probe-photon energy dependence of the amplitude (solid) and the phase (dashed) of the oscillation signal in the induced absorption change calculated from the result depicted in Fig. 2.

the oscillation frequencies and the damping factors. Assuming a sum of the damped cosine function, one can determine the oscillation frequencies and the initial phases of the ruffling and doming modes to be 240 cm⁻¹ and 49°, and 318 cm⁻¹ and 23°, respectively. These results are in good agreement with the corresponding values calculated from the multi-channel detection shown in Fig. 5. Although the contribution of the ISRS cannot be completely ruled out, the phase spectra indicate that the transient oscillations cannot be interpreted only by the ISRS process. Hereafter we shall discuss the contributions of the wave-packet motions in the S₂- and S₁-exciton-state PESs.

In the present system, the S₂-exciton relaxes to the S₁-exciton faster than the disappearance of the wave packet. Thus, the oscillation component at the delay time longer than the S₂-exciton lifetime cannot be attributed to the wave-packet motion on the S₂-exciton-state PES. However, it can be explained as follows by taking account of the wave-packet motion on the S₁-exciton-state PES based on the dynamic intensity borrowing (DIB) mechanism.⁷ A schematic energy diagram is shown in Fig. 6. A vibrational wave packet is launched on the S₂-exciton-state PES by the excitation pulse. Although the S₂-exciton relaxes to the S₁-exciton state through S₂ → S₁ IC, the vibrational coherence is considered to be maintained even on the S₁-exciton-state PES. Since the energy gap between the S₂- and S₁-exciton states is about 6300 cm⁻¹, the IC process results not only from the ruffling and doming modes but also from other several vibrational modes with higher frequencies. Once the wave packet starts to move on the S₁-exciton-state PES, the movement allows the oscillator strength to be transferred from the S₁-exciton state to the S₂-exciton state, or vice versa through DIB mechanism. Therefore, the modulation of

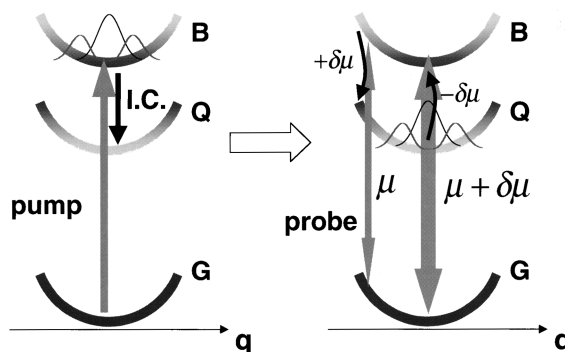


Fig. 6. Schematic energy diagram of the TSPP J-aggregates.

The larger and smaller oscillator strength is indicated as a thick line with partially dark and light parts of the PES of the Q- and B-bands. The left and right sides represent the population distribution before and after the IC, respectively.

the oscillator strength of the S_2 -exciton transition affects the bleaching at the S_2 -exciton state. In the previous study, the wave packet was resonantly photogenerated on the S_1 -exciton-state PES and the modulation of the S_1 -transition was directly monitored by probing the S_1 -transition.⁷ On the other hand, in the present study, the wave packet was generated on the S_1 -exciton-state PES through $S_2 \rightarrow S_1$ IC and the modulation is detected by probing the S_2 -transition. In contrast with the previous study, this can be classified into an indirect observation of the DIB process. The oscillation was more clearly observed in the case of the S_1 -resonant excitation than in the present experiment. It can be explained by the following two reasons. First, the laser spectrum has the peak at the red side of the S_2 -exciton absorption peak; thus the excited vibrational quantum number is smaller than in the previous study. Second, the oscillator strength transferred from the B-transition to the Q-transition (or vice versa) is expected to be equal, based on the DIB theory. Since the stationary absorption of the B-band is more intense than the one of the Q-band, the modulated signal due to the B-transition becomes relatively smaller than the one due to the Q-transition. If the vibrational dephasing could take place due to the $S_2 \rightarrow S_1$ IC, the amplitude of the modulation would be expected to be smaller than the value before the IC. In the present signal-to-noise ratio, such behavior is not clearly time-resolved. Further work is required to investigate this dephasing process.

Conclusion

The S_2 -exciton band of the porphyrin J-aggregates is resonantly photoexcited by 30-fs-laser pulses. The decay-time constant of the slow-decaying component is determined to be 380 ± 10 fs, which is attributed to the $S_2 \rightarrow S_1$ IC. In the transient trace, the oscillating signal is also observed with the 241 ± 4 cm^{-1} and 319 ± 4 cm^{-1} frequencies, which are assigned to the ruffling and the doming modes, respectively. Since the

phase of the oscillation cannot be reproduced only by the ISRS, the contribution of the wave-packet motion on the S_2 - and S_1 -exciton-state PES is also taken into account. Although there is no population in the S_2 -exciton state even after the $S_2 \rightarrow S_1$ IC, the bleaching signal of the S_2 -exciton state is modulated. This is explained by the DIB mechanism, based on which the B-transition is modulated through the wave-packet motion on the Q-band due to the vibronic coupling between the B- and Q-transition.

The work is partly supported by Research for the Future of Japan Society for the Promotion of Science (JSPS-RFTF-97P-00101).

References

- 1 A. H. Zewail, *Science*, **242**, 1645 (1988).
- 2 H. L. Fragnito, J. Y. Bigot, P. C. Becker, and C. V. Shank, *Chem. Phys. Lett.*, **160**, 101 (1989).
- 3 M. J. Rosker, F. W. Wise, and C. L. Tang, *Phys. Rev. Lett.*, **57**, 321 (1986).
- 4 T. Kobayashi and A. Shirakawa, *Chem. Phys. Lett.*, **321**, 385 (2000).
- 5 A. Shirakawa and T. Kobayashi, *Appl. Phys. Lett.*, **72**, 147 (1998).
- 6 A. Sugita, T. Saito, H. Kano, M. Yamashita, and T. Kobayashi, *Phys. Rev. Lett.*, **86**, 2158 (2001).
- 7 H. Kano, T. Saito, and T. Kobayashi, *J. Phys. Chem. B*, **105**, 413 (2001); H. Kano, T. Saito, and T. Kobayashi, *J. Phys. Chem. A*, in press.
- 8 T. Kobayashi, T. Saito, and H. Ohtani, *Nature*, **414**, 531 (2001).
- 9 Y. Shibata, C. Haik, N. Mataga, N. Yoshida, and A. Osuka, "Technical digest of Ultrafast phenomena 2000," TuF44-1/463.
- 10 G. Stock and W. Domcke, *Phys. Rev. A*, **45**, 3032 (1992).
- 11 G. Stock and W. Domcke, *J. Opt. Soc. Am. B*, **7**, 1970 (1990).
- 12 D. J. Kane and R. Torebino, *IEEE J. Quantum Electron.*, **29**, 571 (1993).
- 13 H. Kano and T. Kobayashi, *J. Chem. Phys.*, **116**, 184 (2002).
- 14 D. L. Akins, S. Ozcelik, H. R. Zhu, and C. Guo, *J. Phys. Chem.*, **100**, 14390 (1996).
- 15 L. Dhar, J. A. Rogers, and K. A. Nelson, *Chem. Rev.*, **94**, 157 (1994).
- 16 L. D. Ziegler, R. Fan, A. E. Desrosiers, and N. F. Scherer, *J. Chem. Phys.*, **100**, 1823 (1994).
- 17 I. A. Walmsley, F. W. Wise, and C. L. Tang, *Chem. Phys. Lett.*, **154**, 315 (1989).
- 18 I. A. Walmsley and C. L. Tang, *J. Chem. Phys.*, **92**, 1568 (1990).
- 19 A. T. N. Kumar, F. Rosca, A. Widom, and P. M. Champion, *J. Chem. Phys.*, **114**, 701 (2001).
- 20 F. W. Wise, M. J. Rosker, G. L. Millhauser, and C. L. Tang, *IEEE J. Quantum Electron.*, **QE-23**, 1116 (1987).